Paleobiology, 46(1), 2020, pp. 1–22
DOI: 10.1017/pab.2019.35

PALEOBIOLOGY
A PUBLICATION OF THE Paleontological SOCIETY

Article

A framework for the integrated analysis of the magnitude, selectivity, and biotic effects of extinction and origination

Andrew M. Bush, Steve C. Wang, Jonathan L. Payne, and Noel A. Heim

Abstract.—The taxonomic and ecologic composition of Earth's biota has shifted dramatically through geologic time, with some clades going extinct while others diversified. Here, we derive a metric that quantifies the change in biotic composition due to extinction or origination and show that it equals the product of extinction/origination magnitude and selectivity (variation in magnitude among groups). We also define metrics that describe the extent to which a recovery (1) reinforced or reversed the effects of extinction on biotic composition and (2) changed composition in ways uncorrelated with the extinction. To demonstrate the approach, we analyzed an updated compilation of stratigraphic ranges of marine animal genera. We show that mass extinctions were not more selective than background intervals at the phylum level; rather, they tended to drive greater taxonomic change due to their higher magnitudes. Mass extinctions did not represent a separate class of events with respect to either strength of selectivity or effect. Similar observations apply to origination during recoveries from mass extinctions, and on average, extinction and origination were similarly selective and drove similar amounts of biotic change. Elevated origination during recoveries drove bursts of compositional change that varied considerably in effect. In some cases, origination partially reversed the effects of extinction, returning the biota toward the pre-extinction composition; in others, it reinforced the effects of the extinction, magnifying biotic change. Recoveries were as important as extinction events in shaping the marine biota, and their selectivity deserves systematic study alongside that of extinction.

Andrew M. Bush. Department of Geosciences and Department of Ecology and Evolutionary Biology, University of Connecticut, 354 Mansfield Road, Unit 1045, Storrs, Connecticut 06269. E-mail: andrew.bush@uconn.edu

Steve C. Wang. Department of Mathematics and Statistics, Swarthmore College, Swarthmore, Pennsylvania 19081. E-mail: scwang@swarthmore.edu

Jonathan L. Payne. Department of Geological Sciences, Stanford University, Stanford, California 94305. E-mail: jlpayne@stanford.edu

Noel A. Heim. Department of Earth and Ocean Sciences, Tufts University, Lane Hall, Medford, Massachusetts 02155. E-mail: noel.heim@tufts.edu

Accepted: 11 September 2019
Data available from the Dryad Digital Repository: https://doi.org/10.5061/dryad.mv97842

Introduction

Paleontologists have studied the dynamics of extinction and origination in the fossil record in great detail, usually with a focus on the magnitude of biodiversity loss or gain (e.g., Newell 1967; Raup and Sepkoski 1982; Benton 1995; Bambach 2006; Alroy 2008). However, the effects of mass extinctions on biotic composition and ecosystem structure do not necessarily scale directly with magnitude, such that magnitude is an incomplete measure of an event's impact on the history of life (Droser et al. 2000; McGhee et al. 2004, 2012; Christie et al. 2013). Magnitude and effect can be discordant if extinction events vary in selectivity, where selectivity describes variation in extinction magnitude among taxonomic or functional groups or with respect to some parameter, such as body size or geographic range (e.g., Jablonski and Raup 1995; Jablonski 1996; Kiessling and Aberhan 2007; Payne and Finnegan 2007; Rivadeneira and Marquet 2007; Friedman 2009; Harnik 2011; Heim and Peters 2011; Powell and MacGregor 2011; Harnik et al. 2012; Vilhena et al. 2013; Payne et al. 2016b). Selective events will alter biotic composition, because taxa that experience higher extinction magnitude will decline as a proportion of the surviving biota, while those that experience lower extinction magnitude will increase proportionally (Fig. 1). Extinction and origination will have a greater effect on composition as either magnitude or selectivity increases (Fig. 1) (Payne et al. 2016a).

0094-8373/20

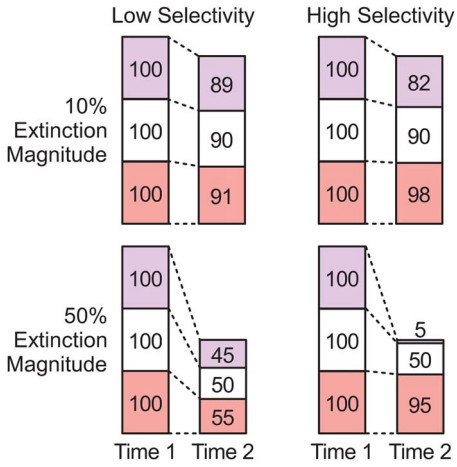

FIGURE 1. Simple hypothetical example of extinction selectivity with three clades. Numbers indicate species richness before and after an extinction. The combination of high selectivity and high magnitude (bottom right) will lead to large changes in relative taxonomic richness between the clades.

Patterns of extinction selectivity for individual events have received considerable attention, often as a means of evaluating or understanding proposed kill mechanisms (e.g., Kitchell et al. 1986; Knoll et al. 1996, 2007; Smith and Jeffery 1998; Lockwood 2003; Leighton and Schneider 2008; Powell 2008; Clapham and Payne 2011; Alegret et al. 2012; Finnegan et al. 2012; Clapham 2017; Penn et al. 2018). Likewise, selectivity has been evaluated for a number of parameters across broader spans of time, permitting comparisons of mass extinctions with one another and with background intervals (e.g., Payne and Finnegan 2007; Janevski and Baumiller 2009; Kiessling and Simpson 2011; Bush and Pruss 2013; Payne et al. 2016a; Reddin et al. 2019). However, an exact quantitative relationship among magnitude, selectivity, and compositional change has never been derived.

Here, we show that the effects of extinction or origination on biotic composition (C), construed as change in the proportional diversity of a set of clades or functional groups, equals the product of extinction/origination magnitude (M) and selectivity (S) under specific definitions of these parameters. We use this quantitative framework to examine a series of questions about biodiversity dynamics in marine animals: (1) Are mass extinctions more selective than background intervals, and do they drive more taxonomic change? In other words, does the magnitude of an event predict the strength of its effects on biotic composition (cf. Droser et al. 2000; McGhee et al. 2004, 2012; Christie et al. 2013)? (2) Do mass extinctions form a separate class of events from background intervals with respect to selectivity or effect (cf. Wang 2003)? (3) On average, is extinction more selective than origination, and does it drive greater amounts of taxonomic change? (4) Do changes in biotic composition driven by origination during recoveries reverse or reinforce the changes driven by mass extinction? The answers to these questions will help provide a richer view of the ways in which extinction and origination shaped the biosphere through geologic time.

Methods

Extinction

We use the per-stage version of Foote's boundary-crosser metric for extinction magnitude (cf. Foote 2003): $q = -\ln[x_{bt}/(x_{bt} + x_{bL})]$, where x_{bt} is the number of taxa crossing the bottom and top boundaries of a time interval and x_{bL} is the number that cross only the bottom boundary (see Table 1 for a listing of abbreviations). The boundary-crosser metric can be standardized by dividing by time-interval duration (Foote 1999, 2000), which will provide an unbiased estimate of the average magnitude during a time interval (Foote 2000). This standardization is beneficial if magnitude is constant or does not vary much within time intervals, whereas the per-stage metric will increase as interval length increases. However, if extinction primarily occurs as pulses within time intervals, as argued by Foote (2005), then the per-stage metric will describe the magnitude of those pulses, whereas the time-standardized metric will vary with interval length (e.g., an extinction pulse would appear half as severe if it were in a time interval twice as long). As we are focused mostly on mass extinctions, we use the per-stage metric, but one could also use the standardized version. Real data undoubtedly reflect a mix of pulsed and background extinction (Stanley 2016), which could

TABLE 1. Definitions of variables.

Variable	Definition
x_{bt}	Number of genera crossing the bottom and top boundaries of a time interval
x_{bL}	Number of genera crossing only the bottom boundary of a time interval
x_{Ft}	Number of genera crossing only the top boundary of a time interval
a_i	Pre-extinction richness of clade i
b_i	Postextinction richness of clade i
q_i	Extinction magnitude of clade i
p_i	Origination magnitude of clade i
n	Number of clades or other groups of interest
$\vec{d}_{ext}$	Vector describing change in richness and composition due to extinction
$\vec{d}_{orig}$	Vector describing change in richness and composition due to origination
$\vec{d}_{net}$	Vector describing change in richness and composition due to extinction and origination
$\vec{m}_{ext}$	Component of $\vec{d}_{ext}$ related to change in total richness
$\vec{c}_{ext}$	Component of $\vec{d}_{ext}$ related to change in the relative richnesses of clades
θ	Angle describing the degree to which clades differ in extinction magnitude
M_{ext}	Overall magnitude of extinction
M_{orig}	Overall magnitude of origination
M_{net}	Overall magnitude of the change in richness due to extinction and origination
C_{ext}	Amount of change in biotic composition due to extinction
C_{orig}	Amount of change in biotic composition due to origination
C_{net}	Amount of change in biotic composition due to extinction and origination
S_{ext}	Selectivity of extinction, equals C_{ext}/M_{ext}
S_{orig}	Selectivity of origination, equals C_{orig}/M_{orig}
$\vec{C}_{ext}$	Vector describing change in biotic composition due to extinction, including amount and direction of change
$\vec{C}_{orig}$	Vector describing change in biotic composition due to origination, including amount and direction of change
$\vec{C}_{net}$	Vector describing change in biotic composition due to both extinction and origination, including amount and direction of change
γ	Angle between $\vec{C}_{ext}$ and $\vec{C}_{orig}$ when placed tip to tail; describes extent to which changes in biotic composition due to extinction and origination are synergistic or antagonistic
r_{pq}	Correlation between q_i and p_i
R_{in}	Reinforcement index, describes the extent to which the changes in biotic composition caused by an extinction were reinforced versus reversed by origination during the recovery
R_{sh}	Reshaping index, describes the relative amount of change in composition driven by origination during a recovery that is uncorrelated with changes driven by the extinction

potentially be accounted for in future analyses. In our preliminary example presented in the "Results," we combine some short stages to form longer (and more standardized) time intervals to help ameliorate the potential weaknesses of the per-stage metric.

The framework derived here also applies to other metrics that treat extinction on a similar scale. In particular, Alroy's gap-filler metric (Alroy 2014, 2015) may be preferable, because it corrects for sampling heterogeneities that may influence the value of q. However, we present the derivation of the method using q, because it is straightforward, and we use q for the preliminary analysis for consistency with the derivation.

Magnitude and Change in Composition.—The boundary-crosser metric q can be rewritten as $\ln(x_{bt} + x_{bL}) - \ln(x_{bt})$, where $x_{bt} + x_{bL}$ and x_{bt} describe pre- and postextinction richness, considering the set of taxa that enters a time interval. For simplicity, we define $a = \ln(x_{bt} + x_{bL})$ and $b = \ln(x_{bt})$, such that $q = a - b$. Given n clades or other groups of interest, we define $a_1 \ldots a_n$ and $b_1 \ldots b_n$ to be the log-transformed pre- and postextinction richnesses of clades 1 through n. Extinction intensities are defined by $q_1 \ldots q_n$, where $q_i = a_i - b_i$.

In Figure 2A, a and b are plotted for two clades. Total change in the biota is represented by the diagonal vector $\vec{d}_{ext}$, which connects the initial composition (black circle) and the final composition (white circle). (Throughout the manuscript, the subscripts "ext" and "orig" will indicate extinction and origination, variables with arrows will denote vectors [e.g., $\vec{m}$], and variables without arrows will denote scalars or lengths of vectors [e.g., m is the length of $\vec{m}$]). The two clades have the same initial richness ($a_1 = a_2$), but $q_1 = 1.0$ and $q_2 = 2.0$, so the first clade fell in richness by a factor of e and the second clade fell by a factor of e^2. The slope of $\vec{d}_{ext}$ is $q_2/q_1 = 2.0$; the extent to which this slope differs from 1.0 is one measure of selectivity (variation in extinction intensity among clades). If the vector $\vec{d}_{ext}$ had a different length but the same slope, the ratio of q_2 to q_1 would be the same, meaning that selectivity was constant, although the magnitude of extinction would be different.

In Figure 2B, the same data are shown along with solid gray diagonal lines that describe sets of points for which the sum of the logged richness values is constant (e.g., [2,0], [1,1], and [0,2]). For purposes of this derivation, we use this sum as a measure of total diversity.

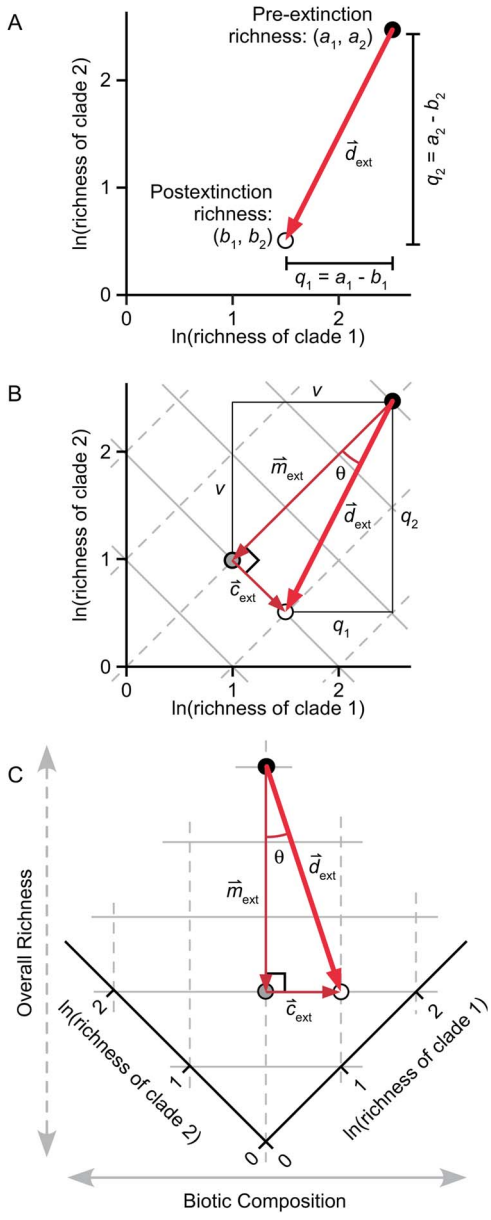

FIGURE 2. Derivation of metrics for extinction magnitude, selectivity, and change in composition. A, Logged richness values for two hypothetical clades. Vector $\vec{d}_{ext}$ represents the overall change in richness and composition of the fauna, and q_1 and q_2 are the boundary-crosser extinction magnitudes for the two clades. B, Same data as in A. The diagonal solid gray lines describe sets of points for which the sum of the logged richness values is constant, and the diagonal dashed gray lines describe sets of points where their difference is constant. Here, $\vec{m}_{ext}$ is the component of $\vec{d}_{ext}$ parallel to the dashed gray lines, representing change in total richness, and $\vec{c}_{ext}$ is the component of $\vec{d}_{ext}$ parallel to the solid gray lines, representing change in the relative richness of the two clades. θ is the angle between $\vec{m}_{ext}$ and $\vec{d}_{ext}$. C, Same as B, rotated 45° counterclockwise so that the horizontal and vertical axes correspond to measures of biotic composition and total richness, respectively.

Normally, of course, total diversity would be calculated as the sum of unlogged values, but this is not possible while working in log space, as required for this derivation. We discuss the potential limitations imposed by this approach under "Additional Discussion of Parameters."

The dashed gray diagonal lines in Figure 2B, whose slopes equal 1.0, describe sets of points for which the difference between the logged richness values of the two clades is constant, indicating that the two clades maintain constant relative richness in arithmetic space. For example, if the difference between two logged richness values is 1.0, then one clade has e times more taxa than the other. The difference in logged richness is a natural measure of biotic composition—that is, the relative taxonomic richnesses of clades.

The diagonal lines in Figure 2B define a set of orthogonal axes that permit one to separate change in total richness from change in relative richness among groups, thus separating the magnitude and compositional effects of an extinction event. In Figure 2C, the diagram from Figure 2B is rotated 45° counterclockwise so that these parameters correspond to the vertical and horizontal axes. In this example, $q_1 \neq q_2$, so there are components of change that are parallel to both the dashed and solid gray lines, which are denoted by $\vec{m}_{ext}$ and $\vec{c}_{ext}$ (Fig. 2B,C). Thus, m_{ext} (the length of vector $\vec{m}_{ext}$) is a measure of the magnitude of the extinction, construed as the change in the sum of the logged richness values of the clades, and c_{ext} (length of $\vec{c}_{ext}$) is a measure of the amount of compositional change driven by the extinction, construed as change in the relative richnesses of the clades. Although m_{ext} and q_i both relate to extinction magnitude, they indicate different aspects: q_i describes the extinction magnitude of individual clades, whereas m_{ext} is a measure of total extinction magnitude (Table 1).

To derive a value for m_{ext}, first note that the dot product of two vectors ($\vec{x}$ and $\vec{y}$) can be calculated two ways. First, $\vec{x} \cdot \vec{y}$ equals $xy\cos(\theta)$, where and x and y are the lengths of the vectors and θ is the angle between them. Second, $\vec{x} \cdot \vec{y}$ equals $\Sigma x_i y_i$, where x_i and y_i are the components of $\vec{x}$ and $\vec{y}$ in each of the n dimensions (all summations are from $i = 1$ to $i = n$, where n is the

number of clades and thus dimensions). Thus, $xy\cos(\theta)$ equals $\Sigma x_i y_i$. The components of $\vec{d}_{ext}$ in the n dimensions are the q_i, whereas $\vec{m}_{ext}$ has the same component in each dimension, labeled v in Figure 2B. Replacing $\vec{x}$ and $\vec{y}$ with $\vec{m}_{ext}$ and $\vec{d}_{ext}$ gives us $m_{ext}d_{ext}\cos(\theta) = \Sigma v q_i = v\Sigma q_i$. Cos(θ) can be replaced with m_{ext}/d_{ext}, because $\vec{m}_{ext}$ and $\vec{d}_{ext}$ form the adjacent side and hypotenuse of a right triangle, which gives us $m_{ext}^2 = v\Sigma q_i$. By the Pythagorean theorem, we know that $m_{ext} = \sqrt{nv^2}$, which rearranges to $v = m_{ext}/\sqrt{n}$. Replacing v gives us $m_{ext}^2 = (m_{ext}/\sqrt{n})(\Sigma q_i)$, which simplifies to $m_{ext} = \Sigma q_i/\sqrt{n}$.

The amount of change in composition, c_{ext}, is the component of change that is parallel to the solid gray lines, equivalent to the distance between the gray circle and the white circle in Figure 2B,C. The white circle is located at (b_1, b_2), which can also be written as $(a_1 - q_1, a_2 - q_2)$, or as $(a_1 - q_1, \ldots, a_n - q_n)$ for n taxa. The length of line segment v equals $m_{ext}/\sqrt{n} = \Sigma q_i/n = \bar{q}$, so the coordinates of the gray point are $(a_1 - \bar{q}, \ldots, a_n - \bar{q})$. The distance between the white and gray circles is then $\sqrt{\sum[(a_i - \bar{q}) - (a_i - q_i)]^2}$, or $\sqrt{\sum(q_i - \bar{q})^2}$.

Thus, we have shown that for magnitude and change in composition, $m_{ext} = \Sigma q_i/\sqrt{n}$ and $c_{ext} = \sqrt{\sum(q_i - \bar{q})^2}$. If we rescale these values by dividing by $\sqrt{n}$, they become

$$M_{ext} = \sum \frac{q_i}{n} = \bar{q} \quad (1)$$

$$C_{ext} = \sqrt{\sum \frac{(q_i - \bar{q})^2}{n}} \quad (2)$$

where M_{ext} and C_{ext} are the rescaled values of m_{ext} and c_{ext}. Thus, the mean of the extinction magnitudes of the individual clades is a measure of the overall magnitude M_{ext} of the extinction event, and the standard deviation of the extinction intensities (calculated as a population, not a sample) is a measure of the amount of change in composition, C_{ext}. Rescaling by $\sqrt{n}$ means that M_{ext} is measured on the same scale as clade-level extinction magnitude, and it permits direct comparisons when the number of clades varies. C_{ext} is a Euclidean distance between the log-transformed composition of pre- and postextinction biotas, similar to some metrics of dissimilarity among ecological communities (e.g., Faith et al. 1987; Legendre and Legendre 2012).

Selectivity.—In Figure 2B,C, the angle θ is a measure of the extent to which $q_1 \neq q_2$; that is, a measure of selectivity. Rather than using θ itself as the selectivity metric, it is more convenient to use tan(θ), which equals c_{ext}/m_{ext} by definition (Fig. 2B,C). Because C_{ext} and M_{ext} are rescaled by the same factor from c_{ext} and m_{ext}, tan(θ) also equals C_{ext}/M_{ext}. For our purposes, using tan(θ) is effectively equivalent to using θ; the two quantities are monotonically related when $0° < \theta < 90°$, and they are nearly linearly related when $\theta < 45°$, which should generally be true in real data sets. If $q_1 = q_2$, θ and tan(θ) are zero (no selectivity), and as the extinction intensities become more dissimilar, θ and tan(θ) increase (selectivity increases).

If we define selectivity of extinction (S_{ext}) to equal tan(θ), then

$$S_{ext} = C_{ext}/M_{ext} \quad (3)$$

$$C_{ext} = S_{ext}M_{ext} \quad (4)$$

Thus, selectivity is the amount of biotic change divided by extinction magnitude, and, equivalently, the amount of biotic change equals selectivity times magnitude. S_{ext} is the coefficient of variation of the extinction intensities of the individual clades, or the standard deviation divided by the mean. The coefficient of variation is a common way of measuring variation that accounts for differences in the mean; here, selectivity is a measure of the amount of compositional change relative to the overall extinction magnitude. The Supplementary Appendix and Supplementary Figure 1 describe a number of hypothetical extinction scenarios that combine different values of M_{ext}, S_{ext}, and C_{ext}.

Accounting for Time-Interval Duration.—As discussed earlier, the boundary-crosser extinction magnitude (as defined here) is sometimes divided by time-interval duration (Δt) in an attempt to correct for variations in duration. Although we do not use this correction here,

it is compatible with our metrics for magnitude, selectivity, and change in composition. The mean and standard deviation of $(q_1/\Delta t, \ldots, q_i/\Delta t)$ equal the mean and standard deviation of $(q_1, \ldots, q_i)$ divided by Δt, so $M_{ext}/\Delta t$ and $C_{ext}/\Delta t$ are the duration-corrected metrics for magnitude and change in composition. Selectivity (S_{ext}) remains the same, because Δt cancels out when $C_{ext}/\Delta t$ is divided by $M_{ext}/\Delta t$.

Origination and Net Change

Magnitude, selectivity, and change in composition can be calculated for origination simply by replacing extinction intensities with origination intensities in equations (1) and (2), yielding the parameters M_{orig}, S_{orig}, and C_{orig}. Origination intensity for individual clades is calculated as $p = -\ln[x_{bt}/(x_{bt} + x_{Ft})] = \ln(x_{bt} + x_{Ft}) - \ln(x_{bt})$, where x_{bt} is number of taxa crossing the bottom and top boundaries of a time interval and x_{Ft} is the number that cross only the top boundary (Foote 1999, 2000) (Table 1). The derivation follows Figure 2, except that the vector representing diversity change ($\vec{d}_{orig}$) would point to the upper right quadrant instead of the lower left quadrant in Figure 2A,B. An example is shown in rotated view in Figure 3.

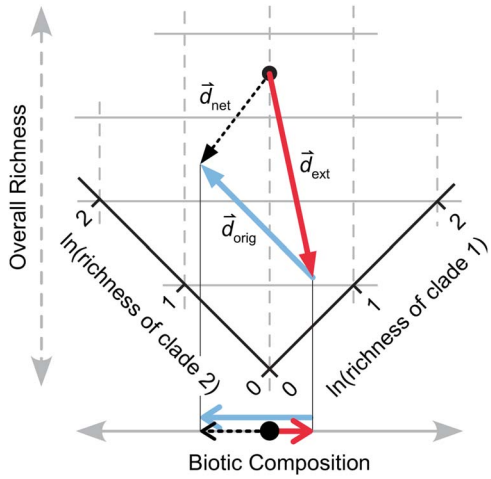

FIGURE 3. Summing the effects of extinction ($\vec{d}_{ext}$) and origination ($\vec{d}_{orig}$). The logged richness values of two clades are shown, rotated as in Fig. 2C so that the horizontal and vertical axes correspond to biotic composition and overall richness, respectively. Net change ($\vec{d}_{net}$) in diversity is the vector sum of $\vec{d}_{ext}$ and $\vec{d}_{orig}$. The three vectors are projected onto the biotic composition axis at the bottom of the panel.

The net change in the richness of group i due to both extinction and origination is $p_i - q_i = [\ln(x_{bt} + x_{Ft}) - \ln(x_{bt})] - [\ln(x_{bt} + x_{bL}) - \ln(x_{bt})] = \ln(x_{bt} + x_{Ft}) - \ln(x_{bt} + x_{bL})$, with positive values indicating an increase in total richness and negative values a decrease. Net magnitude of richness change (M_{net}) and net change in composition (C_{net}) can be calculated as the mean and population standard deviation of these negative and positive values. However, we do not define a corresponding selectivity metric, because coefficients of variation are not used for variables that take both positive and negative values. In the analyses presented in the "Results," $\vec{C}_{net}$ is calculated by comparing extinction in one interval and origination in the following interval, an approach that evaluates the total change driven by an extinction and its recovery. One could also calculate $\vec{C}_{net}$ based on origination and extinction values from the same interval.

C_{ext}, C_{orig}, and C_{net} describe the amount of change in composition, but change in composition also has a direction that describes which clades increase in proportional richness and which decrease. Direction of change is important in understanding how extinction and origination combine to drive biotic change—if the clades that have high extinction magnitude have equivalently high origination magnitude, then the effects of origination and extinction on composition will cancel out. Conversely, if clades that suffer high extinction also suffer low origination, then biotic change will be much more significant. Thus, examining change in composition as vectors is essential to understanding the ultimate effects of extinction and origination.

When plotting the logged richnesses of multiple taxa, the vector representing total diversity change ($\vec{d}_{net}$, black arrow in Fig. 3) is the sum of the vectors representing the changes driven by extinction ($\vec{d}_{ext}$, red arrow) and origination ($\vec{d}_{orig}$, blue arrow). In Figure 3, these three vectors are projected onto the biotic composition axis (bottom), where the black arrow is still the sum of the blue and red. These arrows have lengths of $C_{ext}\sqrt{n}$, $C_{orig}\sqrt{n}$, and $C_{net}\sqrt{n}$; that is, the values for change in composition before rescaling by dividing by $\sqrt{n}$. With two clades, biotic composition can be described

unidimensionally (Fig. 3), and one could use positive and negative numbers to express direction of change.

For n clades, an $(n-1)$-dimensional space is needed to represent biotic composition. Thus, the solid gray line representing biotic composition in Figure 3 would expand to a two-dimensional plane for three clades, as shown in Figure 4A. The red, blue, and black vectors represent the change in composition driven by extinction, origination, and their sum ($\vec{C}_{ext}$, $\vec{C}_{orig}$, and $\vec{C}_{net}$); that is, they are the higher-dimensional analogues of the arrows on the gray axis below Figure 3, rescaled by $\sqrt{n}$. They represent both the amount of change in composition (their lengths equal C_{ext}, C_{orig}, and C_{net}) and the relative direction of change. Additional clades would increase the dimensionality of this space, but two vectors and their sum always lie in a single plane, so higher-dimensional cases can be represented in two dimensions. For ease of comparison, we always show $\vec{C}_{ext}$ directed upward with its base at the origin and $\vec{C}_{orig}$ directed to the right with its base at the tip of $\vec{C}_{ext}$, as in Figure 4A.

With three or more taxa, $\vec{C}_{ext}$ and $\vec{C}_{orig}$ can form any angle from 0° to 180°, denoted here as γ (Fig. 4A). If γ is large, $\vec{C}_{net}$ will be longer than either $\vec{C}_{ext}$ or $\vec{C}_{orig}$ (Fig. 4B, scenarios *i* and *ii*). If γ is small, however, $\vec{C}_{ext}$ and $\vec{C}_{orig}$ will to some extent cancel out, and $\vec{C}_{net}$, their sum, will be shorter than either or both of them (Fig. 4B, scenarios *iii* and *iv*). Given the right combination of angle and vector lengths, $\vec{C}_{net}$ could have the same length as either $\vec{C}_{orig}$ and $\vec{C}_{ext}$ or both (Fig. 4A). The angle γ can be calculated from the correlation coefficient between the clade-level origination and extinction magnitudes (r_{pq}):

$$\gamma = \cos^{-1}(r_{pq}) \tag{5}$$

The derivation for equation (5) is shown in the Appendix, as are the derivations for the following equations for calculating C_{net}, which might be convenient in some cases:

$$C_{net} = \sqrt{C_{orig}^2 + C_{ext}^2 - 2C_{orig}C_{ext}r_{pq}} \tag{6}$$

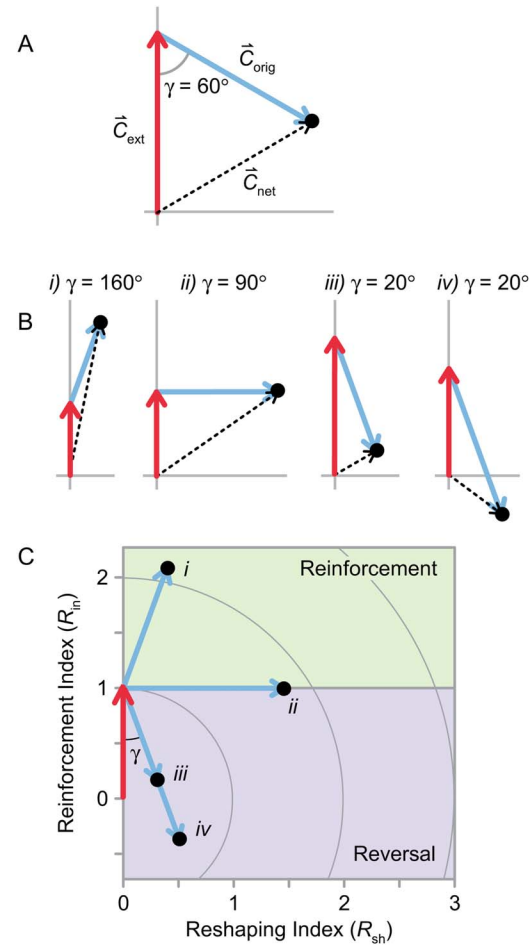

FIGURE 4. Change in biotic composition for three or more clades. A, Net change in composition ($\vec{C}_{net}$) is the vector sum of $\vec{C}_{ext}$ and $\vec{C}_{orig}$, and γ is the angle between $\vec{C}_{ext}$ and $\vec{C}_{orig}$ when they are placed tip to tail. B, Various values of $\vec{C}_{ext}$, $\vec{C}_{orig}$, $\vec{C}_{net}$, and γ. When γ is large (*i*, *ii*), $\vec{C}_{net}$ is longer than $\vec{C}_{ext}$ or $\vec{C}_{orig}$ (i.e., the effects of extinction and origination on biotic composition are synergistic). When γ is small (*iii*, *iv*), $\vec{C}_{ext}$ and $\vec{C}_{orig}$ will cancel out to some extent when summed to form $\vec{C}_{net}$. C, The sets of vectors from B are rescaled so that $\vec{C}_{ext}$ has unit length. $\vec{C}_{net}$ vectors have been excluded for clarity; however, the values of C_{net} relative to C_{ext} are described by the circles, with values indicated on the vertical axis. The reinforcement index (R_{in}) and reshaping index (R_{sh}) correspond to the vertical and horizontal axes, respectively.

$$C_{net} = \sqrt{C_{orig}^2 + C_{ext}^2 - 2C_{orig}C_{ext}\cos(\gamma)} \tag{7}$$

In the analyses presented in the "Results," $\vec{C}_{net}$ is calculated by comparing extinction in one interval with origination in the following interval, an approach that evaluates the total

change driven by an extinction and its recovery. In this case, γ describes the degree to which extinctions and recoveries have similar or opposite effects on biotic composition.

Reinforcement, Reversal, and Reshaping of Biotic Change

We define two additional parameters, the reinforcement index (R_{in}) and the reshaping index (R_{sh}):

$$R_{in} = 1 - (C_{orig}/C_{ext})\cos(\gamma) \quad (8)$$

$$R_{sh} = (C_{orig}/C_{ext})\sin(\gamma) \quad (9)$$

In Figure 4C, each set of vectors from Figure 4B is rescaled so that $C_{ext} = 1$, which means that R_{in} is displayed on the vertical axis and R_{sh} is displayed on the horizontal axis.

The reinforcement index describes the extent to which the changes in biotic composition caused by extinction were reinforced versus reversed by origination during the recovery (i.e., it is the component of $\vec{C}_{orig}$ that is parallel to $\vec{C}_{ext}$; Fig. 4C). For example, if a mass extinction caused the proportion of mollusks to rise relative to the proportion of brachiopods (i.e., the mollusk extinction magnitude was lower), then $R_{in} > 1$ would indicate that mollusks also gained relative to brachiopods during the recovery (i.e., the mollusk origination magnitude was higher, and $\gamma > 90°$; example *i* in Fig. 4B,C). If $R_{in} = 1$, then the two clades did not change in relative richness during the recovery ($\gamma = 90°$; scenario *ii* in Fig. 4B,C). $R_{in} < 1$ would indicate that brachiopods increased at the expense of mollusks during the recovery, at least partially reversing the effects of the extinction ($\gamma < 90°$; scenario *iii* in Fig. 4B,C). $R_{in} = 0.0$ indicates that all changes were reversed, and $R_{in} < 0.0$ means that the recovery reversed all changes and caused the fauna to change in the opposite way (e.g., brachiopods recovered so strongly that they ended up relatively more diverse than they were in the pre-extinction fauna; scenario *iv* in Fig. 4B,C). R_{in} is scaled relative to C_{ext}, so $R_{in} = 2.0$ means that the recovery doubled the change caused by extinction.

The reshaping index describes the amount of change in composition driven by origination that is uncorrelated with the change driven by extinction (i.e., the component of $\vec{C}_{orig}$ perpendicular to $\vec{C}_{ext}$; Fig. 4C). If, as described earlier, mollusks gained relative to brachiopods as a result of extinction, then reshaping during the recovery could include echinoderms gaining at the expense of cnidarians, or any other change that did not involve mollusks relative to brachiopods. Like R_{in}, R_{sh} is scaled relative to C_{ext}; $R_{sh} = 1.0$ indicates that reshaping accomplished as much biotic change as the extinction itself.

Error Bars

To account for uncertainty in values of magnitude, selectivity, and change in composition due to random sampling error, we calculated errors bars around our parameter estimates using Bayesian 95% credible intervals (see Supplementary Appendix for R code). Each of the three parameter estimates is based on the extinction magnitudes of the clades in a given interval (the q_i). These extinction magnitudes are subject to binomial random variability, and this variability must be accounted for in the error bars. Calculating frequentist confidence intervals in this situation is not straightforward, because selectivity and change in composition are complicated functions of the extinction magnitudes. We therefore used a Bayesian simulation-based approach. For each clade in each time interval, we used a standard Bayesian model for estimating the binomial probability of a genus going extinct (Wang 2010). We used a uniform distribution as the prior, combining it with fossil occurrence data to generate a posterior distribution for the probability of extinction. We then randomly sampled 1000 values from this posterior distribution, which we used to estimate the posteriors for the q_i (or p_i) in each time interval. Using the posteriors for all q_i in a time interval, we derived the posterior distributions of magnitude, selectivity, and change in composition for that interval. We then took the middle 95% of each posterior, giving us 95% equal-tail credible intervals. These credible intervals are analogous to frequentist confidence intervals and quantify the uncertainty in the estimated values of magnitude, selectivity, and change in composition, accounting for variability due

to clade size and uncertainty in the underlying extinction rates.

Additional Discussion of Parameters

Magnitude.—Our metrics for extinction and origination magnitude give each clade equal weight, regardless of individual richness. In contrast, the overall extinction or origination intensity for a biota is typically calculated by lumping all taxa into a single pool, such that more diverse clades more strongly influence the value. If one considers clades to be the units of interest in the analysis, then giving clades equal weight is legitimate. In any case, for the example presented on marine animals (see "Results"), M_{ext} and M_{orig} are highly correlated with magnitude calculated by pooling all taxa ($r^2 \geq 0.95$ with $p << 0.01$ for raw data and first differences), suggesting that this difference in approach will not present practical difficulties in many cases. Excluding clades with very low richness (see "Small Sample Sizes") should also strengthen this correspondence. However, the correlation between M and q or p based on the pooled fauna would be weaker if clades differed greatly in both richness and extinction/origination magnitude. In that case, the methods outlined here may not be well suited to the data.

Change in Composition.—Change in composition is calculated as a Euclidean distance based on a measure of the relative number of species or genera within clades, much like how one might calculate dissimilarity among communities or fossil assemblages using the relative number of individuals within species (e.g., Faith et al. 1987; Legendre and Legendre 2012). Thus, our C metrics have straightforward, intuitive interpretations. To further satisfy ourselves that our C_{ext} and C_{orig} are reasonable, we compared values calculated from the marine animal data set (see "Results") with values of Bray-Curtis dissimilarity calculated on proportional logged richness data for pre- and postextinction faunas and pre- and postorigination faunas. For raw data and first differences for both C_{ext} and C_{orig}, $r^2 \geq 0.92$ with $p << 0.01$. The two metrics are calculated quite differently (Bray-Curtis is nonmetric and non-Euclidean), but we present the comparison simply to show that C captures the same basic information as a metric that is commonly used in studies of ecological and paleoecological gradients (Clarke and Warwick 2001; Bush and Brame 2010; Legendre and Legendre 2012) and in studies of faunal change through time (Clapham 2015).

Small Sample Sizes.—It may be difficult to interpret M, C, and S when some clades have very low richness, because stochastic variations could lead to greatly different parameter estimates. At the extreme, a clade that only has one genus will have an observed extinction intensity of either zero or infinity, regardless of the underlying probability of extinction. Credible intervals, as implemented here, should help in the interpretation of parameter values based on low-richness clades by highlighting the high uncertainty associated with such values. In the analysis presented in the "Results," we also excluded individual clades from time intervals in which richness was extremely low ($x_{bt} + x_{bL} < 8$ genera for extinction; $x_{bt} + x_{Ft} < 8$ genera for origination).

Low Magnitude.—Quantification of selectivity will be inherently uncertain when extinction/origination magnitude is very low. S_{ext} and S_{orig} are equivalent to coefficients of variation, which become sensitive to small changes in the denominator (M_{ext} or M_{orig}) as it approaches zero (cf. Gould 1984). Thus, selectivity could take on anomalously high and/or uncertain values when magnitude is extremely low. To the extent that variations in extinction/origination intensity among groups are driven by random sampling error, credible intervals like those used here will assist in quantifying this uncertainly (e.g., selectivity is high, but the credible interval extends to low values). However, it is likely that some variation in extinction/origination intensity among groups is driven by other types of heterogeneity in the data, such as variations in sampling and preservation, which may not be captured by our methodology and which are more difficult to model. Difficulty in precisely quantifying selectivity when magnitude is low is a problem for other selectivity metrics as well, because no technique will accurately quantify variation among variables whose values are so small that errors overwhelm the signal.

Infinite Values.—When a clade goes completely extinct, the calculated extinction intensity equals infinity with the boundary-crosser metric, and M_{ext} and C_{ext} will also equal infinity (likewise for origination at a clade's earliest appearance). Infinite values are inherently awkward to evaluate, and they are misleading in many cases. To the extent that calculated extinction intensity is an estimate of the underlying probability that individual taxa in a clade go extinct, boundary-crosser values of infinity imply that all members of a clade are absolutely guaranteed to die. In reality, the underlying probability is probably less than 100%, corresponding to a high but not infinite boundary-crosser value. The sample analysis presented in the "Results" was conducted at the phylum level, so no group ever went completely extinct and infinite magnitudes were not an issue.

If infinite values do occur in an analysis, several measures could be taken. Excluding clades from time intervals in which they have few genera, as discussed earlier, should help, because infinite values may be most common in these cases. In addition, our Bayesian credible interval routine provides finite error bars even when all component taxa in a group go extinct. To get point estimates for *M* and *C*, one could use the mean or median of the posterior distribution for each parameter.

Comparisons with Other Methods.—Used individually, *M* and *C* should generally produce results that are similar to existing metrics, as seen earlier. This is not unexpected, as reasonable methods that measure the same phenomenon should produce broadly similar results. The primary benefits of the framework described here are that magnitude, selectivity, and change in composition are measured on compatible scales, and clear relationships among them are derived from first principles. Also, the framework permits the development of new kinds of metrics, such as R_{in} and R_{sh}, that can be applied to macroevolutionary questions. The parameters are simple to calculate once clade-level values for extinction/origination have been determined (eqs. 1, 2).

Our selectivity metric, *S*, describes variation in extinction magnitude among a set of groups. Multiple logistic regression, which is commonly used in selectivity studies, can measure selectivity with respect to other types of variables, such as binary traits (e.g., benthic vs. pelagic) or continuous traits (e.g., body size). It can also evaluate multiple predictors at once. Thus, the two methods are useful in different circumstances. Payne et al. (2016a) calculated the "influence" of an extinction event on a biota as the geometric mean of selectivity (logistic regression coefficient) and magnitude (percent loss), which is somewhat similar to the relationship we derive here. However, they did not provide a detailed justification for combining these parameters.

Alroy (2000, 2004) also developed a set of methods that are similar in some respects to the one presented here. The "proportional volatility index" measures change in taxonomic composition, similar to our *C* metrics, although calculated differently (Alroy 2000). The "proportional volatility *G* statistic" quantifies the extent to which observed intensities of extinction and/or origination for taxa within a particular time interval differ from those expected given the average value for each group among time intervals and the overall intensity within the interval of interest (Alroy 2000, 2004). Both metrics were applied to overall changes in composition between adjacent time intervals, although they could be split into contributions from extinction and origination.

Like our selectivity metric, the *G* statistic measures variation in turnover among groups, but the methods are different in important ways. The *G* statistic quantifies the extent to which the extinction magnitudes of taxa in a particular time interval differ from their expected values given long-term averages. In contrast, S_{ext} simply measures variation in extinction magnitude among taxa within a time interval, standardized by overall magnitude, without comparison to long-term average values. Thus, the metrics are designed to answer different questions. For the questions that we are investigating, our methods have the added benefit that *S*, *C*, and *M* are related (eqs. 3, 4).

Data

We applied these methods to the Phanerozoic marine animal fossil record, which has

been the subject of extensive work on extinction and origination magnitude (e.g., Raup and Sepkoski 1982; Bambach et al. 2004; Foote 2005, 2007; Stanley 2007; Alroy 2008) and some on selectivity (Payne and Finnegan 2007; Kiessling and Simpson 2011; Bush and Pruss 2013; Payne et al. 2016a). For this initial trial, we analyzed an updated version of Sepkoski's (2002) compendium (Heim et al. 2015). Phanerozoic-scale patterns of origination and extinction are generally similar in the Paleobiology Database (Alroy 2014). We included six diverse phyla that provide mostly continuous series of extinction intensities spanning most of the Phanerozoic at the stage level: Arthropoda, Brachiopoda, Chordata, Cnidaria, Echinodermata, and Mollusca.

We combined consecutive stages in several cases in which stage length and/or number of extinctions was low. We excluded the Cambrian and Tremadocian (earliest Ordovician), because more than one phylum was below our sample-size cutoff of eight genera for $x_{bt} + x_{bL}$ and/or $x_{bt} + x_{Ft}$. This cutoff is somewhat arbitrary, but it allows us to include at least five phyla for all time intervals. The Cnidaria were excluded from the analysis for several time intervals in which they did not meet this cutoff (Floian/Dapingian, Lopingian, Early Triassic, Anisian). Values of M, S, and C were highly similar when based on five versus six phyla for time intervals that met the sample-size cutoff (r^2 between 0.90 and 0.98).

Of the 56 time intervals in the analysis, we highlight 13 that encompass the "big five" mass extinctions of Raup and Sepkoski (1982), the Early Triassic, and most of the minor mass extinctions listed by Bambach (2006) (excluding the Pliensbachian–Toarcian event, which did not clearly stand out in the analysis). For analyses of origination, we highlighted the time intervals that followed these 13, because elevated origination followed many mass extinctions (e.g., Stanley 2007; Alroy 2008; Foote 2010). Table 2 lists the specific time intervals used to characterize each event.

As noted earlier, C_{net}, γ, R_{in}, and R_{sh} were calculated based on C_{ext} in one interval and C_{orig} in the following interval, an approach that evaluates the total change driven by an extinction event and by origination during the subsequent recovery. For these parameters, the Cnidaria had to be excluded from an additional time interval (Capitanian), because the subsequent interval (Lopingian) did not meet the sample-size cutoff.

TABLE 2. Extinction events and recovery intervals highlighted in the analysis. The big five mass extinctions of Raup and Sepkoski (1982) are marked in bold.

	Event	Extinction interval	Recovery interval
E	Eocene	Late Eocene	Oligocene
K	**Cretaceous/ Paleogene**	Maastrichtian	Paleocene
C	Cenomanian	Cenomanian	Turonian
t	Tithonian	Tithonian	Berriasian–Valanginian
T	**Triassic/Jurassic**	Norian–Rhaetian	Hettangian–Sinemurian
e	Early Triassic	Early Triassic	Anisian
P	**Permian/Triassic**	Lopingian	Early Triassic
G	Guadalupian (Capitanian)	Capitanian	Lopingian
S	Serpukhovian	Serpukhovian	Bashkirian
D_3	Devonian/ Carboniferous	Famennian	Tournaisian
D_2	**Frasnian/ Famennian**	Frasnian	Famennian
D_1	Givetian	Givetian	Frasnian
O	**Late Ordovician**	Katian–Hirnantian	Llandovery

Results

Extinction

The Ordovician through Neogene history of extinction magnitude M_{ext} (Fig. 5A), which is the average of the clade-level values of q, was similar to the results of previous analyses of marine fossil animals (e.g., Alroy 2008, 2014) (see Supplementary Tables 1–3 for raw results of analyses). Mass extinctions, construed as either the big five or as all events listed in Table 2, were not significantly different in selectivity S_{ext} from background intervals, at least in this preliminary phylum-level analysis ($p > 0.05$, Mann-Whitney U-test) (Figs. 5B and 6C, Table 3). The Late Ordovician mass extinction and the Givetian had low selectivity, the Early Triassic had extremely high selectivity, and all other mass extinctions were fairly similar (Fig. 5B). A number of background intervals had high selectivity (>0.75) and low magnitude (Fig. 5D), but M_{ext} and S_{ext} were not correlated ($r^2 = 0.03$, $p > 0.05$).

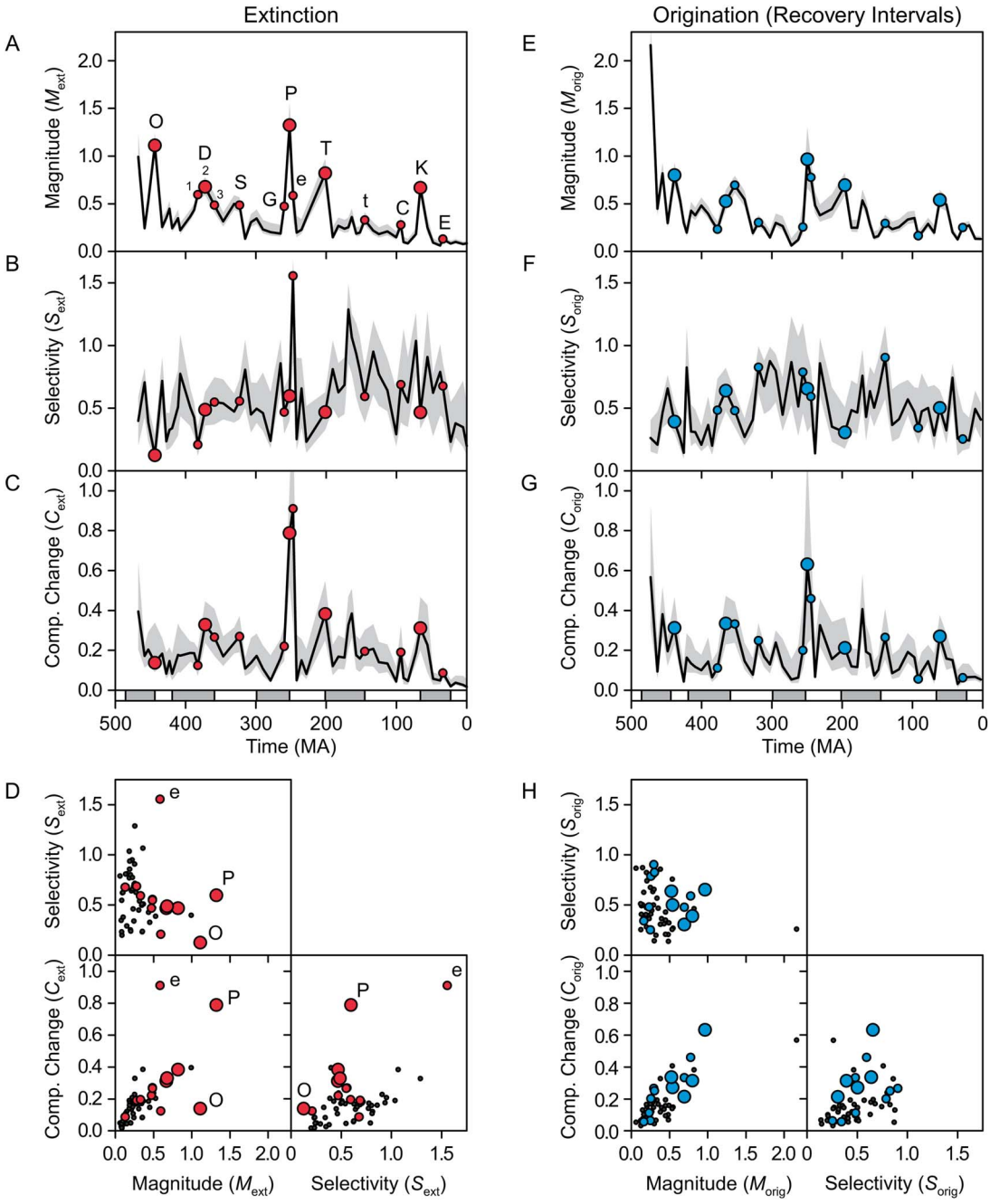

FIGURE 5. Magnitude, selectivity, and the resulting change in biotic composition ("Comp. Change") for extinction (A–D) and origination (E–H) in marine animals. The gray bands show 95% credible intervals. For extinction (A–D), the larger circles mark the big five mass extinctions, and the smaller circles mark minor extinction events. For origination (E–H), the circles mark recovery intervals (i.e., the time intervals following the extinctions). Points are plotted at the ends of time intervals for extinction and at their midpoints for origination. The highlighted extinction intervals are labeled in A: O, Late Ordovician; D_1, Givetian; D_2, Frasnian/Famennian; D_3, Devonian/Carboniferous; S, Serpukhovian; G, Guadalupian; P, Permian/Triassic; e, Early Triassic; T, Triassic/Jurassic; t, Tithonian; C, Cenomanian; K, Cretaceous/Paleogene; E, Eocene.

TABLE 3. The *p*-values from statistical tests of single parameters. The first two columns report *p*-values from two-sided Mann-Whitney *U*-test comparisons of mass extinctions and all other time intervals, with mass extinctions encompassing either the big five events of Raup and Sepkoski (1982) or all events ("All MEs") listed in Table 2. The final two columns report *p*-values from Silverman's critical bandwidth test for multimodality. Double asterisks (**) mark *p*-values less than 0.01, and single asterisks (*) mark *p*-values less than 0.05.

Parameter	Big five vs. other intervals	All MEs vs. other intervals	Multimodal (raw data)	Multimodal (logged data)
M_{ext}	** < 0.01	** < 0.01	0.80	0.67
M_{orig}	** < 0.01	* 0.04	0.26	0.44
S_{ext}	0.18	0.60	0.63	0.69
S_{orig}	0.688	0.18	0.62	0.91
C_{ext}	* 0.01	** < 0.01	0.37	0.80
C_{orig}	** < 0.01	** < 0.01	0.63	0.78
C_{net}	* 0.04	** < 0.01	0.56	0.89
γ	0.07	0.75	0.48	0.59
R_{in}	0.07	0.961	0.44	0.29
R_{sh}	0.90	0.22	0.41	0.87
C_{orig}/C_{ext}	0.40	0.73		

By far, extinction forced the greatest change in composition during the end-Permian event and the Early Triassic (Fig. 5C), with the other mass extinctions causing, at most, half as much change. Change in composition was significantly greater for mass extinctions than for other intervals (Table 3, Fig. 6E), and M_{ext} and C_{ext} were correlated more strongly than S_{ext} and C_{ext} ($r^2 = 0.45$ vs. 0.24, $p << 0.01$ for both; Fig. 5D). Given its extremely low selectivity, the Late Ordovician extinction caused little change in composition for its magnitude, whereas highly selective extinction in the Early Triassic caused an unusually large amount of change (after removing these two intervals, r^2 between M_{ext} and C_{ext} rose to 0.73).

Origination

Overall, origination magnitude and change in composition were elevated during recovery intervals (cf. Alroy 2008; Foote 2010), although selectivity was not (Table 3, Figs. 5E–G and 6B, D,F; note that origination is highlighted for time intervals immediately following extinctions). In fact, C_{orig} was significantly correlated with C_{ext} from the previous time interval ($r^2 =$ 0.45 for raw data and 0.23 for first differences, $p << 0.01$ for both). The recoveries that followed the end-Permian extinction and the Early Triassic had high magnitude of origination and reasonably high selectivity, and as a result, they drove more change in composition than the other recoveries (Fig. 5E–G). Origination magnitude and change in composition were also high for the first interval in the time series (Floian/Dapingian), representing the continuing Ordovician radiation (Fig. 5E,G). As was the case for extinction, change in composition was more strongly correlated with magnitude than with selectivity ($r^2 = 0.59$ with $p << 0.01$ vs. $r^2 = 0.12$ with $p = 0.01$; Fig. 5H). Overall, values of *M*, *S*, and *C* did not significantly differ between extinction and origination (Fig. 6A–F, Table 4).

Net Change

C_{net} (change in composition driven by extinction plus origination in the following time interval) was significantly different for mass extinctions than for other intervals (Table 3, Fig. 6G). Overall, C_{net} was not significantly greater than C_{ext}, although it was significantly (though only slightly) greater than C_{orig} (Table 4, Fig. 6E–G). C_{net} was higher than C_{ext} for some extinctions (e.g., Ordovician, Famennian, and Eocene extinctions) and lower for others (e.g., Permian, Triassic, and Cretaceous extinctions; Early Triassic) (Fig. 7A). The vector representations of $\vec{C}_{ext}$, $\vec{C}_{orig}$, and $\vec{C}_{net}$ show how the former case is associated with a large angle (γ) between $\vec{C}_{ext}$ and $\vec{C}_{orig}$, whereas the latter is associated with a small angle (Fig. 7B). This angle did not differ significantly between mass extinctions and background intervals (Table 3, Fig. 6H). The observed values of γ were also no different from those obtained by randomly pairing sets of q_i and p_i from different time intervals or from random

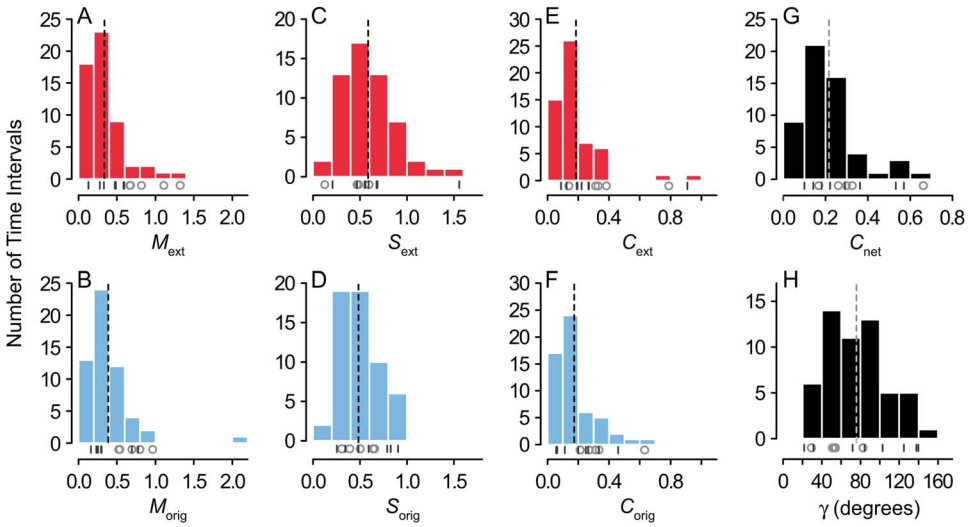

FIGURE 6. Histograms of extinction and origination magnitude (A,B), selectivity (C,D), and change in composition (E,F); total change in composition (G); and the angle γ between the vectors $\vec{C}_{ext}$ and $\vec{C}_{orig}$ (H). Dashed vertical lines mark mean values. Beneath the histograms, open circles mark the values of the big five mass extinctions, and dashes mark the positions of the minor mass extinctions listed in Table 2.

TABLE 4. Results of two-sided Mann-Whitney *U*-test comparisons of two parameters. Single asterisks (*) mark *p*-values less than 0.05.

Parameter 1	Parameter 2	*p*-value
M_{ext}	M_{orig}	0.18
S_{ext}	S_{orig}	0.06
C_{ext}	C_{orig}	0.64
C_{ext}	C_{net}	0.09
C_{orig}	C_{net}	* 0.01

pairing among the 13 mass extinctions and recoveries listed in Table 2 (Mann-Whitney *U*-test, $p > 0.05$).

Reinforcement, Reversal, and Reshaping

In Figure 7C, the reinforcement and reshaping indices (R_{in} and R_{sh}) for all time intervals are plotted as in Figure 4C, but with the blue arrows removed for clarity. The recoveries from the big five mass extinctions are all characterized by partial reversal ($0 < R_{in} < 1$); that is, some of the change in biotic composition driven by extinction was reversed by origination during the recovery. In the case of the Frasnian extinction (D_2), almost all of the change was reversed (R_{in} near zero). R_{in} describes the amount of change during a recovery relative to the value of C_{ext}, not the absolute magnitude of change, which is shown in Figure 7B. Thus, mass extinctions and recoveries accomplished large amounts of total change (C_{net}) despite this tendency toward reversal.

Reinforcement occurred during the recoveries from several of the minor extinctions (Givetian, Famennian, Tithonian, and Eocene). Background intervals (black dots) were not significantly different from mass extinctions on either axis (Mann-Whitney *U*-test; Table 3), reflecting the fact that mass extinctions and background intervals did not differ significantly in γ or C_{orig}/C_{ext} (Table 3).

The average value of R_{in} was 0.76, with a bootstrapped 95% confidence interval of (0.59, 0.93) (bootstrapping based on 10,000 iterations). In other words, the mean of R_{in} was significantly different from 1.0, indicating a tendency toward some reversal of biotic change driven by extinction. However, for the big five events, the average R_{in} was lower, with a mean of 0.49 and a 95% confidence interval of (0.29, 0.65). The average amount of reshaping was 0.98, with a 95% confidence interval of (0.79, 1.19). There was an unusually large amount of reshaping during the recovery from the Late Ordovician extinction (Fig. 7C).

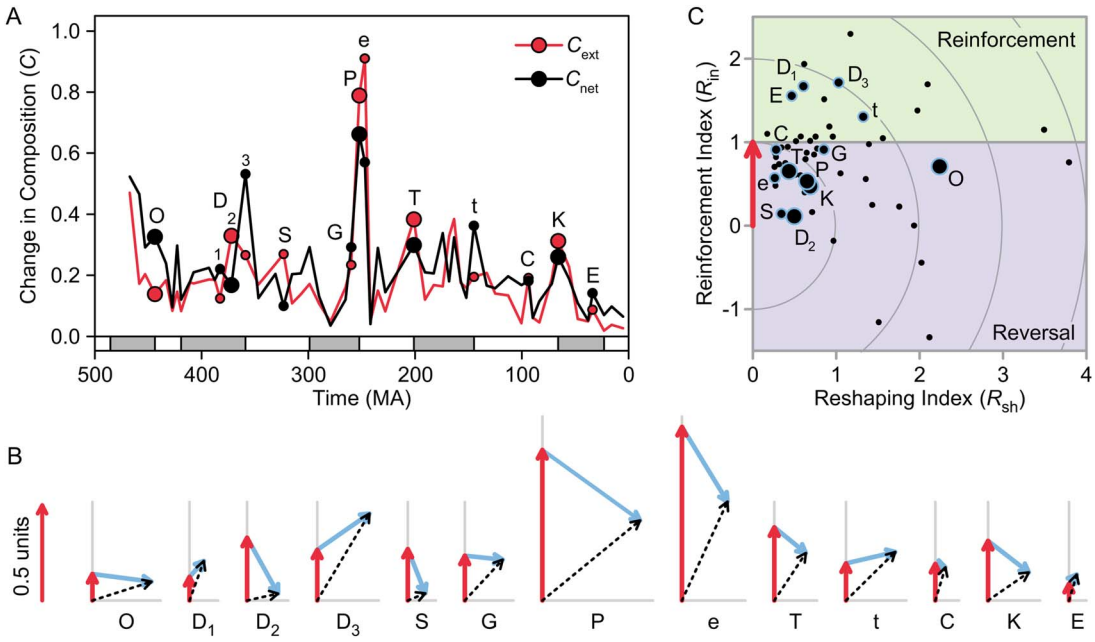

FIGURE 7. Net change in biotic composition calculated with a one-interval lag between extinction and origination. A, Comparison of net change (C_{net}) and change driven by extinction (C_{ext}). B, Vector representations of the change in composition driven by extinction ($\vec{C}_{ext}$, red), origination ($\vec{C}_{orig}$, blue), and their sum ($\vec{C}_{net}$, black), oriented so that $\vec{C}_{ext}$ points up. $\vec{C}_{ext}$ was highest during the late Permian and Early Triassic due to high extinction magnitude in the former and high selectivity in the latter (Fig. 5A–C). C, Reinforcement and reshaping indices (R_{in} and R_{sh}). In A and C, large circles mark the big five mass extinctions, and small circles mark minor mass extinctions. O, Late Ordovician; D_1, Givetian; D_2, Frasnian/Famennian; D_3, Devonian/Carboniferous; S, Serpukhovian; G, Guadalupian; P, Permian/Triassic; e, Early Triassic; T, Triassic/Jurassic; t, Tithonian; C, Cenomanian; K, Cretaceous/Paleogene; E, Eocene.

Discussion

General Patterns

Mass Extinctions versus Background Intervals.—On average, mass extinctions and their recoveries drove more biotic change than background intervals, a result that holds when Raup and Sepkoski's (1982) big five events are compared with other intervals or when all highlighted intervals in Table 2 are compared with other intervals (Figs. 5, 6, Table 3). However, there is considerable overlap in C_{ext} and in C_{orig} between mass extinctions and other intervals due to low selectivity of some mass extinctions (e.g., Late Ordovician and Givetian; Fig. 5A–C) and the inclusion of extinction events that represent local maxima in M_{ext} during times of low background values, particularly during the Mesozoic and Cenozoic (Fig. 5A). Some events in this latter group, particularly the Cenomanian and Eocene, also show up as local maxima in C_{ext} (Fig. 5C).

Mass extinctions and their recoveries did not differ significantly from background intervals in selectivity, and change in composition C_{ext} was correlated more strongly with magnitude M_{ext} than selectivity S_{ext} (Fig. 5D). Thus, overall, major extinction events drove larger-than-normal changes in biotic composition, primarily due to greater magnitude. This result seemingly contrasts with demonstrations that mass extinction magnitude and ecological effects are not strongly related (Droser et al. 2000; McGhee et al. 2004, 2012; Christie et al. 2013), possibly implying that taxonomic and ecological effects have different relationships with magnitude. However, the correlation between magnitude and ecological effects would be more apparent if background time intervals were included in the comparisons of McGhee et al. (2012) and others. For comparison, r^2 between M_{ext} and C_{ext} in our data is 0.28 when only the big five extinctions are included and 0.45 for all intervals. In other

words, the influence of magnitude on effect (however it is measured) will be less apparent when magnitude is restricted to a narrower range (the restricted-range problem; e.g., Bland and Altman [2011]).

Despite the correlation between M_{ext} and C_{ext}, extremely low or high selectivity did cause some events to have unusually weak or strong effects on phylum-level biotic composition. In particular, the Late Ordovician extinction had very low selectivity (Fig. 5B), leading to little high-level taxonomic change (Fig. 5C). As documented previously, the Late Ordovician event also did not have large-scale effects on ecosystem structure (e.g., Droser et al. 2000; McGhee et al. 2004, 2012; Christie et al. 2013; Krug and Patzkowsky 2015), although tropical and deep-water taxa were affected disproportionately (Finnegan et al. 2012, 2016; Congreve et al. 2018).

Conversely, selectivity was unusually high during the Early Triassic (cf. Song et al. 2013; Payne et al. 2016a; Clapham 2017), leading to large amounts of taxonomic change; in fact, C_{ext} was higher in this interval than in any other (Fig. 5B,C). Some taxa had high rates of turnover at this time (Brayard et al. 2009; Romano et al. 2013), and continued environmental disturbance and destabilization of ecosystems may have preferentially affected some taxa (Payne et al. 2004; Galfetti et al. 2007; Chen and Benton 2012; Romano et al. 2013; Song et al. 2014; Clarkson et al. 2015; Petsios et al. 2019; Pietsch et al. 2019). However, due to low richness in the Early Triassic, the error bars on C_{ext} are quite wide, with the lower bound equaling only 0.34 (Fig. 5C). Thus, any conclusions about this time interval have a great degree of uncertainty, even before one takes into account other kinds of sampling problems that may be particularly acute (e.g., Erwin and Hua-Zhang 1996; Wignall and Benton 1999).

Many of the highest values for S_{ext} correspond to low values of M_{ext} (<0.4) (Fig. 5D), although the two variables were not strongly correlated ($r^2 = 0.03$, $p > 0.05$). As noted in "Methods," this could reflect the fact that $S_{ext} = C_{ext}/M_{ext}$, so small values of M_{ext} could inflate values of S_{ext} (cf. Gould 1984). If sampling is random, then the error bars should overlap zero if this is the case, but heterogeneities in preservation and sampling could elevate values of S_{ext} without being reflected in the error bars. However, the high values of S_{ext} at fairly low values of M_{ext} may reflect reality. For one thing, the pattern is not as severe for origination (Fig. 5H), as would be expected if sampling alone were the cause. Also, high values of S_{ext} are concentrated in the Jurassic and Cretaceous, and there are some consistent patterns among phyla during this interval that cannot be explained by sampling error; for example, brachiopods tend to have one of the highest extinction magnitudes (Supplementary Table 3).

In fact, high selectivity may be easier to achieve in time intervals with little extinction, because it requires only small absolute variations in magnitude among groups. In contrast, high-magnitude, high-selectivity extinction events may be rare, because magnitude must be extraordinarily high in some groups and extraordinarily low in others, and few kill mechanisms are likely to be so intense yet so focused, at least at this level of analysis. For example, the end-Permian extinction was somewhat selective in our analysis (Fig. 5B), but Penn et al. (2018) found that tolerance to hypoxia and temperature change were not strongly phylogenetically conserved, such that these kill mechanisms affected all phyla to some extent. Likewise, climate change and loss of habitat will not cause highly selective extinctions if phyla are widespread among climate zones and geographic regions (cf. the Late Ordovician extinction). Selectivity is likely to appear stronger at lower taxonomic levels, because lower-level taxa are less likely to have such wide tolerances and distributions.

Separate Class of Events?—Several authors have examined the question of whether mass extinctions represent a separate class of events with respect to extinction magnitude, or whether they merely represent the upper tail of a continuous distribution (e.g., Raup and Sepkoski 1982; Wang 2003; Bambach et al. 2004). As pointed out by Wang (2003), continuity of mass and background extinction can also be examined with respect to cause and effect. We find insufficient evidence to claim discontinuity of effect at the phylum level, in that

C_{ext} is not significantly multimodal according to Silverman's critical bandwidth test (Silverman 1981; Wang 2003) (Fig. 6E, Table 3). Values of C_{ext} for the Permian extinction and Early Triassic appear as outliers in Figures 5C and 6E and could, in theory, represent a second mode, but these two data points were insufficient to establish a pattern.

Mass extinctions could also represent a separate class of events with respect to selectivity (i.e., continuity of selectivity), but S_{ext} was not significantly different during mass extinctions and background events (Fig. 6C, Table 3). This analysis only addresses overall strength of taxonomic selectivity at the phylum level, not the more detailed patterns that may be associated with particular extinction kill mechanisms, such as which specific taxa experience high versus low magnitude of extinction (e.g., McKinney 1987). There was also no evidence of a separate class of events with regard to origination (M_{orig}, S_{orig}, or C_{orig}) or total change in composition (C_{net}) (Fig. 6, Table 3).

Extinction versus Origination.—Given the attention devoted to the selectivity of mass extinctions, as well as the possible links between selectivity and dramatic environmental perturbations, it would not be surprising if extinctions were more selective and drove greater biotic changes than origination. However, overall, extinction and origination were not significantly different in selectivity and biotic effects according to Mann-Whitney *U*-tests (Table 4). Evidently, the two processes are similarly capable of driving biotic change. It is possible that there are more subtle differences between extinction and origination that could represent biologically interesting phenomena. For example, S_{ext} exceeded 0.95 in five time intervals, whereas S_{orig} never did, so perhaps maximum selectivity is slightly higher for extinction than for origination.

Mass Extinctions and Recoveries

As seen here and in previous studies (Stanley 2007; Alroy 2008; Foote 2010), elevated origination magnitude tended to follow mass extinction (Fig. 5E), leading to a recovery of total richness. Recoveries are also characterized by elevated change in composition due to origination, because C_{orig} is correlated with M_{orig} (Fig. 5H). However, the effects of these pulses of change varied considerably among events.

In some cases, the compositional change caused by a mass extinction was largely reversed by the pulse of change during the subsequent recovery. In these cases, the clade-level extinction and origination magnitudes were positively correlated, such that the clades that suffered more also recovered more. The Serpukhovian (S) and Frasnian (D_2) events are the most notable, with values of R_{in} near zero (all change canceled; equivalent to low γ and $C_{net} < C_{ext}$; Fig. 7). The effects of the Permian (P) and Cretaceous (K) mass extinctions were also substantially reversed (~50%; Fig. 7C), as were the effects of extinction during the Early Triassic (e). The Permian extinction and Early Triassic have the highest values for C_{net}, but these values were not dramatically higher than those for other events, in contrast with C_{ext} (Fig. 7A).

In some cases, pulses of origination after mass extinctions did not lead to a "recovery" in biotic composition, in the sense of "a return toward the pre-existing state" (cf. Lockwood 2004, 2005). In a few cases, the recovery reshaped the fauna without substantially reversing or reinforcing the extinction's effects ($R_{sh} > R_{in}$), including the Late Ordovician (O), Guadalupian (G), and Cenomanian (C) events (Fig. 7B,C). In other cases, the phyla that suffered the most in the extinction tended to recover the least, such that the "recovery" actually made the fauna even more dissimilar from its pre-extinction composition (reinforcement, with $R_{in} > 1$ in Fig. 7C). Examples include the Givetian (D_1), Famennian (D_3), and Eocene (E).

On average, about 25% of the change in composition caused by extinction was reversed by origination in the next interval (average $R_{in} = 0.76$). Mild reversal is the average case, because extinction and origination magnitudes are somewhat correlated among phyla (mean $r_{pq} = 0.33$) (e.g., Stanley 1979; Gilinksy 1994). However, randomizing the q_i and p_i among time intervals (or among the 13 events listed in Table 2) does not produce a mean value of γ or r_{pq} that is significantly different from the observed mean, suggesting that, at this level

of analysis, the exact direction of selectivity during an extinction does not substantially affect the direction of selectivity of the recovery. One can expect that, on average, some reversal will occur, but no more than expected given the general differences in volatility among phyla.

Interestingly, there is a hint that the recoveries from the big five mass extinctions might be more predictable than expected by chance alone. Recoveries from these extinctions reversed about half of the change caused by extinction (average $R_{in} = 0.49$), more than is typical for other events (overall, average $R_{in} = 0.76$). Definite conclusions are not possible given the small sample size, and a comparison is not statistically significant ($p = 0.07$, Mann-Whitney *U*-test; Table 3), but it is possible that only large extinctions disrupt the biota enough to affect the selectivity of recovery. If this pattern holds up, it means that large events have less impact on higher-level taxonomic composition than one might expect looking at extinction alone.

Conversely, the high values of reinforcement observed for several minor extinction events indicate that these extinction–recovery couplets are more important for the history of life than would be obvious from analyses of extinction alone. For example, C_{net} for the Famennian extinction (D_3) and subsequent recovery is higher than for any other time interval except the late Permian and Early Triassic (Fig. 7A), a result that reinforces claims of this event's importance (e.g., Sallan and Coates 2010; Sallan et al. 2011; Marynowski et al. 2012; Becker et al. 2016). In contrast, the Frasnian event (D_2) has often been considered one of the big five extinctions, but its taxonomic effects at the phylum level were largely erased by the subsequent recovery. However, one of the most important effects of the extinction—the decimation of reef ecosystems (e.g., Copper 2002)—is largely not captured by our analysis, which did not include sponges or consider ecosystem-level patterns (for other work on the event, see Joachimski and Buggisch 2002; Bambach et al. 2004; Bond and Wignall 2008; Stigall 2012; Bush et al. 2015; Ma et al. 2015).

These results emphasize that the full effects of an extinction–recovery couplet may have a considerable random component. For a given kill mechanism, one might be able to predict how extinction itself will change faunal composition (e.g., Knoll et al. 2007) and that origination will increase afterward, leading to a partial or full recovery of total richness. On average, some of the compositional effects of extinction will be reversed during the recovery (~25% on average, or ~50% for large events), but there is considerable variation around this expectation, with some recoveries reinforcing rather than reversing the effects of extinction (Fig. 7C). Also, there is a considerable amount of reshaping in many cases (Fig. 7C).

Future studies should examine whether the effects of recoveries are more predictable when other parameters are considered (e.g., functional groups; Bush et al. 2007; Novack-Gottshall 2007; Bush and Bambach 2011), or whether recovery dynamics can be predicted based on environmental conditions or ecological dynamics (e.g., Solé et al. 2002; Payne and van de Schootbrugge 2007; Roopnarine et al. 2007; Hull et al. 2011, 2015; Dineen et al. 2014; Foster and Twitchett 2014; Hull 2015; Henehan et al. 2016).

Conclusions

Extinction and origination magnitude only describe changes in the total richness of a biota, but quantifying their effects on the relative diversity of clades or functional groups is essential for understanding ecosystem reorganization and the long-term history of life. The effects of extinction or origination on biotic composition can be defined as the product of extinction/origination magnitude and selectivity ($C = SM$). Within this framework, one can directly quantify the extent to which the effects of extinction and origination were driven by magnitude versus selectivity.

A preliminary application of these methods at the phylum level reveals several insights into the biodiversity dynamics of marine animals; future analyses of finer taxonomic groups or ecological modes of life may provide additional insights. On average, mass extinctions were not more selective than background intervals at the phylum level, such that they tended to cause greater amounts of change in the composition of the fauna due to greater magnitude.

However, biotic change was noticeably greater or less than would be predicted by magnitude for several high- and low-selectivity time intervals (e.g., the Early Triassic and Late Ordovician extinctions, respectively). Mass extinctions did not represent a separate class of events with regard to strength of selectivity or amount of change in composition (i.e., the distribution of values was not significantly bimodal).

Origination magnitude and effect on composition were elevated in the time intervals following mass extinctions, although these recoveries did not represent a separate class of event with respect to magnitude or effect. On average, selectivity of origination was not elevated during recoveries, so the increased effect was driven primarily by increased magnitude. On average, extinction and origination had similar values for magnitude, selectivity, and effect on faunal composition. In other words, extinction and origination drove equivalent amounts of change in the biota.

The reinforcement index (R_{in}) describes the extent to which changes in faunal composition driven by mass extinction events were strengthened by changes driven by origination during the subsequent recovery (i.e., the same groups gained in relative diversity during the extinction and recovery). Extinction–recovery couplets with high R_{in} caused more total change in the biota than would be expected based on extinction alone (e.g., Givetian, Famennian, and Eocene), whereas events with low R_{in} caused less total change, because the effects of extinction were largely reversed during the recovery (e.g., Frasnian and Serpukhovian). On average, recoveries drove mild reversal, because phyla with high extinction rates tended to have high origination rates, but individual events varied widely. Recoveries also caused considerable amounts of biotic change uncorrelated with the changes driven by extinction, as described by the reshaping index (R_{sh}).

These results support the critical role of recoveries from mass extinctions in shaping the history of life and suggest some fruitful avenues for future research. Specifically, is there a general principle that explains the selectivity of recoveries and their effects on biotic composition? Is the selectivity of a recovery closely related to the selectivity of the preceding mass extinction for some level of analysis or set of parameters, or can their dynamics be explained by ecological or environmental conditions?

Acknowledgments

Our thanks to M. Hopkins, M. Clapham, and two anonymous reviewers for valuable feedback on the article. In addition, A.M.B. acknowledges support from National Science Foundation (NSF) grant EAR-1738121, S.C.W. acknowledges funding from Swarthmore College, and J.L.P. acknowledges support from NSF CAREER grant EAR-1151022. S.C.W. thanks William Sparks and Mayank Agrawal for their assistance.

References

Alegret, L., E. Thomas, and K. C. Lohmann. 2012. End-Cretaceous marine mass extinction not caused by productivity collapse. Proceedings of the National Academy of Sciences USA 109:728–732.

Alroy, J. 2000. New methods for quantifying macroevolutionary patterns and processes. Paleobiology 26:707–733.

Alroy, J. 2004. Are Sepkoski's evolutionary faunas dynamically coherent? Evolutionary Ecology Research 6:1–32.

Alroy, J. 2008. Dynamics of origination and extinction in the fossil record. Proceedings of the National Academy of Sciences USA 105:11536–11542.

Alroy, J. 2014. Accurate and precise estimates of origination and extinction rates. Paleobiology 40:374–397.

Alroy, J. 2015. A more precise speciation and extinction rate estimator. Paleobiology 41:633–639.

Bambach, R. K. 2006. Phanerozoic biodiversity mass extinctions. Annual Review of Earth and Planetary Sciences 34:127–55.

Bambach, R. K., A. H. Knoll, and S. C. Wang. 2004. Origination, extinction, and mass depletions of marine diversity. Paleobiology 30:522–542.

Becker, R. T., S. I. Kaiser, and M. Aretz. 2016. Review of chrono-, litho- and biostratigraphy across the global Hangenberg Crisis and Devonian–Carboniferous boundary. *In* R. T. Becker, P. Königshof, and C. E. Brett, eds. Devonian climate, sea level and evolutionary events. Geological Society of London Special Publication 423:355–386.

Benton, M. J. 1995. Diversification and extinction in the history of life. Science 268:52–58.

Bland, J. M., and D. G. Altman. 2011. Correlation in restricted ranges of data. BMJ 342:d556.

Bond, D. P., and P. B. Wignall. 2008. The role of sea-level change and marine anoxia in the Frasnian–Famennian (Late Devonian) mass extinction. Palaeogeography, Palaeoclimatology, Palaeoecology 263:107–118.

Brayard, A., G. Escarguel, H. Bucher, C. Monnet, T. Brühwiler, N. Goudemand, T. Galfetti, and J. Guex. 2009. Good genes and good luck: ammonoid diversity and the end-Permian mass extinction. Science 325:1118–1121.

Bush, A. M., and R. K. Bambach. 2011. Paleoecologic megatrends in marine Metazoa. Annual Review of Earth and Planetary Sciences 39:241–269.

Bush, A. M., and R. I. Brame. 2010. Multiple paleoecological controls on the composition of marine fossil assemblages from the Frasnian (Late Devonian) of Virginia, with a comparison of ordination methods. Paleobiology 36:573–591.

Bush, A. M., and S. B. Pruss. 2013. Theoretical ecospace for ecosystem paleobiology: energy, nutrients, biominerals, and macroevolution. *In* A. M. Bush, S. B. Pruss, and J. L. Payne, eds. Ecosystem paleobiology and geobiology. Paleontological Society Papers 19:1–20.

Bush, A. M., R. K. Bambach, and G. M. Daley. 2007. Changes in theoretical ecospace utilization in marine fossil assemblages between the mid-Paleozoic and late Cenozoic. Paleobiology 33:76–97.

Bush, A. M., J. D. Csonka, G. V. DiRenzo, D. J. Over, and J. A. Beard. 2015. Revised correlation of the Frasnian-Famennian boundary and Kellwasser events (Upper Devonian) in shallow marine paleoenvironments of New York State. Palaeogeography, Palaeoclimatology, Palaeoecology 433:233–246.

Chen, Z.-Q., and M. J. Benton. 2012. The timing and pattern of biotic recovery following the end-Permian mass extinction. Nature Geoscience 5:375.

Christie, M., S. M. Holland, and A. M. Bush. 2013. Contrasting the ecological and taxonomic consequences of extinction. Paleobiology 39:538–559.

Clapham, M. E. 2015. Ecological consequences of the Guadalupian extinction and its role in the brachiopod-mollusk transition. Paleobiology 41:266–279.

Clapham, M. E. 2017. Organism activity levels predict marine invertebrate survival during ancient global change extinctions. Global Change Biology 23:1477–1485.

Clapham, M. E., and J. L. Payne. 2011. Acidification, anoxia, and extinction: a multiple logistic regression analysis of extinction selectivity during the Middle and Late Permian. Geology 39:1059–1062.

Clarke, K. R., and R. M. Warwick. 2001. Change in marine communities: an approach to statistical analysis and interpretation. Primer-E, Plymouth, U.K.

Clarkson, M., S. Kasemann, R. Wood, T. Lenton, S. Daines, S. Richoz, F. Ohnemueller, A. Meixner, S. Poulton, and E. Tipper. 2015. Ocean acidification and the Permo-Triassic mass extinction. Science 348:229–232.

Congreve, C. R., A. Z. Krug, and M. E. Patzkowsky. 2018. Evolutionary and biogeographical shifts in response to the Late Ordovician mass extinction. Palaeontology 62:267–285.

Copper, P. 2002. Reef development at the Frasnian/Famennian mass extinction boundary. Palaeogeography, Palaeoclimatology, Palaeoecology 181:27–65.

Dineen, A. A., M. L. Fraiser, and P. M. Sheehan. 2014. Quantifying functional diversity in pre-and post-extinction paleocommunities: a test of ecological restructuring after the end-Permian mass extinction. Earth-Science Reviews 136:339–349.

Droser, M. L., D. J. Bottjer, P. M. Sheehan, and G. R. McGhee Jr. 2000. Decoupling of taxonomic and ecologic severity of Phanerozoic marine mass extinctions. Geology 28:675–678.

Erwin, D. H., and P. Hua-Zhang. 1996. Recoveries and radiations: gastropods after the Permo-Triassic mass extinction. *In* M. B. Hart, ed. Biotic recovery from mass extinction events. Geological Society of London Special Publication 102:223–229.

Faith, D. P., P. R. Minchin, and L. Belbin. 1987. Compositional dissimilarity as a robust measure of ecological distance. Vegetatio 69:57–68.

Finnegan, S., N. A. Heim, S. E. Peters, and W. W. Fischer. 2012. Climate change and the selective signature of the Late Ordovician mass extinction. Proceedings of the National Academy of Sciences USA 109:6829–6834.

Finnegan, S., C. M. Ø. Rasmussen, and D. A. T. Harper. 2016. Biogeographic and bathymetric determinants of brachiopod extinction and survival during the Late Ordovician mass extinction. Proceedings of the Royal Society of London B 283:20160007.

Foote, M. 1999. Morphological diversity in the evolutionary radiation of Paleozoic and post-Paleozoic crinoids. Paleobiology 25:1–115.

Foote, M. 2000. Origination and extinction components of taxonomic diversity: general problems. Paleobiology 26:74–102.

Foote, M. 2003. Origination and extinction through the Phanerozoic: a new approach. Journal of Geology 111:125–148.

Foote, M. 2005. Pulsed origination and extinction in the marine realm. Paleobiology 31:6–20.

Foote, M. 2007. Extinction and quiescence in marine animal genera. Paleobiology 33:261–272.

Foote, M. 2010. The geological history of biodiversity. Pp. 479–510 *in* M. A. Bell, D. J. Futuyma, W. F. Eanes, and J. S. Levinton, eds. Evolution since Darwin: the first 150 years. Sinauer, Sunderland, Mass.

Foster, W. J., and R. J. Twitchett. 2014. Functional diversity of marine ecosystems after the Late Permian mass extinction event. Nature Geoscience 7:233–238.

Friedman, M. 2009. Ecomorphological selectivity among marine teleost fishes during the end-Cretaceous extinction. Proceedings of the National Academy of Sciences USA 106:5218–5223.

Galfetti, T., P. A. Hochuli, A. Brayard, H. Bucher, H. Weissert, and J. O. Vigran. 2007. Smithian–Spathian boundary event: evidence for global climatic change in the wake of the end-Permian biotic crisis. Geology 35:291–294.

Gilinksy, N. L. 1994. Volatility and the Phanerozoic decline of background extinction intensity. Paleobiology 20:445–458.

Gould, S. J. 1984. Smooth curve of evolutionary rate: a psychological and mathematical artifact. Science 226:994–995.

Harnik, P. G. 2011. Direct and indirect effects of biological factors on extinction risk in fossil bivalves. Proceedings of the National Academy of Sciences USA 108:13594–13599.

Harnik, P. G., C. Simpson, and J. L. Payne. 2012. Long-term differences in extinction risk among the seven forms of rarity. Proceedings of the Royal Society of London B 279:4969–4976.

Heim, N. A., and S. E. Peters. 2011. Regional environmental breadth predicts geographic range and longevity in fossil marine genera. PLoS ONE 6:e18946.

Heim, N. A., M. L. Knope, E. K. Schaal, S. C. Wang, and J. L. Payne. 2015. Cope's rule in the evolution of marine animals. Science 347:867–870.

Henehan, M. J., P. M. Hull, D. E. Penman, J. W. Rae, and D. N. Schmidt. 2016. Biogeochemical significance of pelagic ecosystem function: an end-Cretaceous case study. Philosophical Transactions of the Royal Society of London B 371:20150510.

Hull, P. 2015. Life in the aftermath of mass extinctions. Current Biology 25:R941–R952.

Hull, P. M., R. D. Norris, T. J. Bralower, and J. D. Schueth. 2011. A role for chance in marine recovery from the end-Cretaceous extinction. Nature Geoscience 4:856–860.

Hull, P. M., S. A. Darroch, and D. H. Erwin. 2015. Rarity in mass extinctions and the future of ecosystems. Nature 528:345–351.

Jablonski, D. 1996. Body size and macroevolution. Pp. 256–289 *in* D. Jablonski, D. H. Erwin, and J. H. Lipps, eds. Evolutionary paleobiology. University of Chicago Press, Chicago.

Jablonski, D., and D. M. Raup. 1995. Selectivity of end-Cretaceous marine bivalve extinctions. Science 268:389–391.

Janevski, G. A., and T. K. Baumiller. 2009. Evidence for extinction selectivity throughout the marine invertebrate fossil record. Paleobiology 35:553–564.

Joachimski, M. M., and W. Buggisch. 2002. Conodont apatite $\delta^{18}O$ signatures indicate climatic cooling as a trigger of the Late Devonian mass extinction. Geology 30:711–714.

Kiessling, W., and M. Aberhan. 2007. Geographical distribution and extinction risk: lessons from Triassic–Jurassic marine benthic organisms. Journal of Biogeography 34:1473–1489.

Kiessling, W., and C. Simpson. 2011. On the potential for ocean acidification to be a general cause of ancient reef crises. Global Change Biology 17:56–67.

Kitchell, J. A., D. L. Clark, and A. M. Gombos Jr. 1986. Biological selectivity of extinction: a link between background and mass extinction. Palaios 1:504–511.

Knoll, A. H., R. K. Bambach, D. E. Canfield, and J. P. Grotzinger. 1996. Comparative Earth history and Late Permian mass extinction. Science 273 452–457.

Knoll, A. H., R. K. Bambach, J. L. Payne, S. Pruss, and W. W. Fischer. 2007. Paleophysiology and end-Permian mass extinction. Earth and Planetary Science Letters 256:295–313.

Krug, A. Z., and M. E. Patzkowsky. 2015. Phylogenetic clustering of origination and extinction across the Late Ordovician mass extinction. PLoS ONE 10:e0144354.

Legendre, P., and L. Legendre. 2012. Numerical ecology, 3rd ed. Elsevier, Amsterdam.

Leighton, L. R., and C. L. Schneider. 2008. Taxon characteristics that promote survivorship through the Permian–Triassic interval: transition from the Paleozoic to the Mesozoic brachiopod fauna. Paleobiology 34:65–78.

Lockwood, R. 2003. Abundance not linked to survival across the end-Cretaceous mass extinction: patterns in North American bivalves. Proceedings of the National Academy of Sciences USA 100:2478–2482.

Lockwood, R. 2004. The K/T event and infaunality: morphological and ecological patterns of extinction and recovery in veneroid bivalves. Paleobiology 30:507–521.

Lockwood, R. 2005. Body size, extinction events, and the early Cenozoic record of veneroid bivalves: a new role for recoveries? Paleobiology 31:578–590.

Ma, X., Y. Gong, D. Chen, G. Racki, X. Chen, and W. Liao. 2015. The Late Devonian Frasnian–Famennian Event in South China—patterns and causes of extinctions, sea level changes, and isotope variations. Palaeogeography, Palaeoclimatology, Palaeoecology 448:1–21.

Marynowski, L., M. Zatoń, M. Rakociński, P. Filipiak, S. Kurkiewicz, and T. J. Pearce. 2012. Deciphering the upper Famennian Hangenberg black shale depositional environments based on multi-proxy record. Palaeogeography, Palaeoclimatology, Palaeoecology 346:66–86.

McGhee, G. R., Jr., P. M. Sheehan, D. J. Bottjer, and M. L. Droser. 2004. Ecological ranking of Phanerozoic biodiversity crises: ecological and taxonomic severities are decoupled. Palaeogeography, Palaeoclimatology, Palaeoecology 211:289–297.

McGhee, G. R., Jr., P. M. Sheehan, D. J. Bottjer, and M. L. Droser. 2012. Ecological ranking of Phanerozoic biodiversity crises: the Serpukhovian (early Carboniferous) crisis had a greater ecological impact than the end-Ordovician. Geology 40:147–150.

McKinney, M. L. 1987. Taxonomic selectivity and continuous variation in mass and background extinctions of marine taxa. Nature 325:143–145.

Newell, N. D. 1967. Revolutions in the history of life. *In* J. C. C. Albritton Jr., ed. Uniformity and simplicity: a symposium on the principle of the uniformity of nature. Geological Society of America Special Paper 89:63–91.

Novack-Gottshall, P. M. 2007. Using a theoretical ecospace to quantify the ecological diversity of Paleozoic and modern marine biotas. Paleobiology 33:273–294.

Payne, J. L., and S. Finnegan. 2007. The effect of geographic range on extinction risk during background and mass extinction. Proceedings of the National Academy of Sciences USA 104:10506–10511.

Payne, J. L., and B. van de Schootbrugge. 2007. Life in Triassic oceans: links between planktonic and benthic recovery and radiation. Pp. 165–189 *in* P. G. Falkowski, and A. H. Knoll, eds. Evolution of primary producers in the sea. Academic Press, Burlington, Mass.

Payne, J. L., D. J. Lehrmann, J. Wei, M. J. Orchard, D. P. Schrag, and A. H. Knoll. 2004. Large perturbations of the carbon cycle during recovery from the end-Permian extinction. Science 305:506–509.

Payne, J. L., A. M. Bush, E. T. Chang, N. A. Heim, M. L. Knope, and S. B. Pruss. 2016a. Extinction intensity, selectivity, and their combined macroevolutionary influence in the fossil record. Biology Letters 12:20160202.

Payne, J. L., A. M. Bush, N. A. Heim, M. L. Knope, and D. J. McCauley. 2016b. Ecological selectivity of the emerging mass extinction in the oceans. Science 353:1284–1286.

Penn, J. L., C. Deutsch, J. L. Payne, and E. A. Sperling. 2018. Temperature-dependent hypoxia explains biogeography and severity of end-Permian marine mass extinction. Science 362: eaat1327.

Petsios, E., J. R. Thompson, C. Pietsch, and D. J. Bottjer. 2019. Biotic impacts of temperature before, during, and after the end-Permian extinction: a multi-metric and multi-scale approach to modeling extinction and recovery dynamics. Palaeogeography, Palaeoclimatology, Palaeoecology 513:86–99.

Pietsch, C., K. A. Ritterbush, J. R. Thompson, E. Petsios, and D. J. Bottjer. 2019. Evolutionary models in the Early Triassic marine realm. Palaeogeography, Palaeoclimatology, Palaeoecology 513:65–85.

Powell, M. G. 2008. Timing and selectivity of the Late Mississippian mass extinction of brachiopod genera from the central Appalachian Basin. Palaios 23:525–534.

Powell, M. G., and J. MacGregor. 2011. A geographic test of species selection using planktonic foraminifera during the Cretaceous/Paleogene mass extinction. Paleobiology 37:426–437.

Raup, D. M., and J. J. Sepkoski Jr. 1982. Mass extinctions in the marine fossil record. Science 215:1501–1503.

Reddin, C. J., Á. T. Kocsis, and W. Kiessling. 2019. Climate change and the latitudinal selectivity of ancient marine extinctions. Paleobiology 45:70–84.

Rivadeneira, M. M., and P. A. Marquet. 2007. Selective extinction of late Neogene bivalves on the temperate Pacific coast of South America. Paleobiology 33:455–468.

Romano, C., N. Goudemand, T. W. Vennemann, D. Ware, E. Schneebeli-Hermann, P. A. Hochuli, T. Brühwiler, W. Brinkmann, and H. Bucher. 2013. Climatic and biotic upheavals following the end-Permian mass extinction. Nature Geoscience 6:57–60.

Roopnarine, P. D., K. D. Angielczyk, S. C. Wang, and R. Hertog. 2007. Trophic network models explain instability of Early Triassic terrestrial communities. Proceedings of the Royal Society of London B 274:2077–2086.

Sallan, L. C., and M. I. Coates. 2010. End-Devonian extinction and a bottleneck in the early evolution of modern jawed vertebrates. Proceedings of the National Academy of Sciences USA 107:10131–10135.

Sallan, L. C., T. W. Kammer, W. I. Ausich, and L. A. Cook. 2011. Persistent predator–prey dynamics revealed by mass extinction. Proceedings of the National Academy of Sciences USA 108:8335–8338.

Sepkoski, J. J., Jr. 2002. A compendium of fossil marine animal genera. Bulletins of American Paleontology 363:1–560.

Silverman, B. W. 1981. Using kernel density estimates to investigate multimodality. Journal of the Royal Statistical Society, Series B 43:97–99.

Smith, A. B., and C. H. Jeffery. 1998. Selectivity of extinction among sea urchins at the end of the Cretaceous period. Nature 392:69–71.

Solé, R. V., J. M. Montoya, and D. H. Erwin. 2002. Recovery after mass extinction: evolutionary assembly in large–scale biosphere dynamics. Philosophical Transactions of the Royal Society of London B 357:697–707.

Song, H., P. B. Wignall, J. Tong, and H. Yin. 2013. Two pulses of extinction during the Permian–Triassic crisis. Nature Geoscience 6:52.

Song, H., P. B. Wignall, D. Chu, J. Tong, Y. Sun, H. Song, W. He, and L. Tian. 2014. Anoxia/high temperature double whammy

during the Permian–Triassic marine crisis and its aftermath. Scientific Reports 4:4132.
Stanley, S. M. 1979. Macroevolution: pattern and process. Freeman, San Francisco.
Stanley, S. M. 2007. An analysis of the history of marine animal diversity. Paleobiology Memoirs 4:1–55.
Stanley, S. M. 2016. Estimates of the magnitudes of major marine mass extinctions in earth history. Proceedings of the National Academy of Sciences USA 113:E6325–E6334.
Stigall, A. L. 2012. Speciation collapse and invasive species dynamics during the Late Devonian "mass extinction." GSA Today 22:4–9.
Vilhena, D. A., E. B. Harris, C. T. Bergstrom, M. E. Maliska, P. D. Ward, C. A. Sidor, C. A. E. Strömberg, and G. P. Wilson. 2013. Bivalve network reveals latitudinal selectivity gradient at the end-Cretaceous mass extinction. Scientific Reports 3:1790.
Wang, S. C. 2003. On the continuity of background and mass extinction. Paleobiology 29:455–467.
Wang, S. C. 2010. Principles of statistical inference: likelihood and the Bayesian paradigm. *In* J. Alroy and G. Hunt, eds. Quantitative methods in paleobiology. Paleontological Society Papers 16:1–18.
Wignall, P., and M. Benton. 1999. Lazarus taxa and fossil abundance at times of biotic crisis. Journal of the Geological Society 156:453–456.

Appendix

The derivations for equations (5) to (7) are provided here. The formula for the variance of the sum of two random variables is $\mathrm{Var}(k_1X + k_2Y) = k_1^2\mathrm{Var}(X) + k_2^2\mathrm{Var}(Y) + 2k_1k_2\mathrm{Cov}(X,Y)$, where X and Y are the random variables and k_1 and k_2 are constants. Replacing X with the clade-level origination magnitudes (p_i), Y with the clade-level origination magnitudes (q_i), k_1 with 1, and k_2 with −1, we get $\mathrm{Var}(p_i - q_i) = \mathrm{Var}(p_i) + \mathrm{Var}(q_i) - 2\mathrm{Cov}(p_i,q_i)$. The variances can be replaced with squared values of C_{net}, C_{orig}, and C_{ext}, as these are the standard deviations of $p_i - q_i$, p_i, and q_i, respectively. The covariance of p_i and q_i can be replaced with their standard deviations times their correlation coefficient (r_{pq}), or $C_{\mathrm{orig}}C_{\mathrm{ext}}r_{pq}$. These changes produce the equation $C_{\mathrm{net}}^2 = C_{\mathrm{orig}}^2 + C_{\mathrm{ext}}^2 - 2C_{\mathrm{orig}}C_{\mathrm{ext}}r_{pq}$. Taking the square root of both sides yields equation (6).

By the law of cosines, which generalizes the Pythagorean theorem to non-right triangles, $C_{\mathrm{net}}^2 = C_{\mathrm{orig}}^2 + C_{\mathrm{ext}}^2 - 2C_{\mathrm{orig}}C_{\mathrm{ext}}\cos(\gamma)$ in Figure 4A. Taking the square root of both sides yields equation (7). Comparison of equations (6) and (7) shows that $\cos(\gamma) = r_{pq}$, where r_{pq} is the correlation between the clade-level origination and extinction magnitudes. Taking the inverse cosine of both sides gives $\gamma = \cos^{-1}(r_{pq})$, which is equation (5).